THE EUROPEAN
PHYSICAL JOURNAL PLUS

Regular Article

Coarse-mesh thermal-hydraulics and neutronics coupling for the ALFRED reactor

Francesco Di Lecce[1,a], **Manuele Aufiero**[1], **Stefano Lorenzi**[2], **Paolo Saracco**[3,4], **Alessandro Alemberti**[5]

[1] Milano Multiphysics S.r.l.s., Via Giovanni Durando c/o PoliHub, 39, 20158 Milan, MI, Italy
[2] Department of Energy, Politecnico di Milano, Via La Masa, 34, 20156 Milan, MI, Italy
[3] INFN - Sezione di Genova, Via Dodecaneso, 33, 16146 Genoa, GE, Italy
[4] Centro Fermi, Piazza del Viminale, 1, 00184 Roma, Italy
[5] Ansaldo Nucleare S.p.A., Corso M. F. Perrone, 25, 16152 Genoa, GE, Italy

Abstract Among the six advanced reactor systems identified by the Generation IV International Forum, the lead fast reactor (LFR) has been considered as one of the most promising future nuclear power plants. Among the LFR designs, Ansaldo Nucleare, as coordinator of the Lead-cooled European Advanced DEmonstration Reactor project, proposes Advanced Lead Fast Reactor European Demonstrator (ALFRED) as LFR demonstrator, which is the study object of the present paper. A multiphysics model for the ALFRED core is developed and presented in this paper, which couples neutronics and thermal hydraulics. The first physics is solved with neutron transport Monte Carlo simulations, while temperatures and the lead density are updated with coarse-mesh-based finite volume method CFD runs. The proposed model focuses on the adoption of spatially non-uniform temperature distributions of materials to compute better on-the-fly estimations of nuclides cross sections and thence a more accurate neutron physics description.

1 Introduction

Lead-cooled fast reactors (LFRs) are one of the six nuclear technologies identified by the Generation IV International Forum (GIF) [1]. Lead-based coolants show several attractive properties (e.g., the absence of exothermic reactions with water, high thermal capacity and low neutron moderation) which encourages researches and developments of LFR commercial plants and demonstrators.

Starting from April 2010, the LEADER (Lead-cooled European Advanced DEmonstration Reactor) project, in the frame of EU 7th FP [2], started to develop a conceptual level of an European LFR industrial-sized plant and of a scaled demonstrator called ALFRED (Advanced Lead Fast Reactor European Demonstrator) [3]. ALFRED will show the feasibility of the LFR technology for use in a future commercial power plant. In December 20,

[a] e-mail: francesco.dilecce@milanomultiphysics.com

2013, a consortium between Italy's National Agency for New Technologies, Energy and the Environment (ENEA) and Ansaldo Nucleare S.p.A., as well as Romania's Nuclear Research Institute (Institutul de Cercetari Nucleare, ICN), has been formally set up to implement the construction of ALFRED in Romania.

The present work is focused on the multiphysics description of the ALFRED core. The interactions between neutronics and thermal hydraulics are solved iteratively, in order to evaluate the material temperatures, the lead density and the power distribution within the reactor. The neutronics is solved with a continuous-energy Monte Carlo code for particle transport, while thermal hydraulics is solved with a finite volume method computational fluid dynamics model.

Specifically, the model intends to perform a more accurate neutronics description: The nuclide cross sections are evaluated on the fly, i.e., during the transport of neutrons in the system, and on spatially non-uniform temperature distributions of coolant and pin materials.

The choice of a Monte Carlo code for the neutronics modeling is based on the possibility to computationally scale the problem and solve it on multiple parallel processors, following a broader ongoing development project being carried out by the authors.

The paper is organized as follows. Firstly, a brief overview of the ALFRED layout and core lattice is given. Then, the multiphysics model is described and the main results are depicted and commented. Finally, a scalability analysis is implemented to test the code efficiency in using an increasing number of parallel cores.

2 Reactor description

ALFRED is a small-size (300 MWth) pool-type LFR. Its primary system current configuration is depicted in Fig. 1 [3]. All the major reactor primary system components, including the core, primary pumps and steam generators (SGs), are contained within the reactor vessel, being located in a large lead pool inside the reactor tank. The coolant flows upward from the
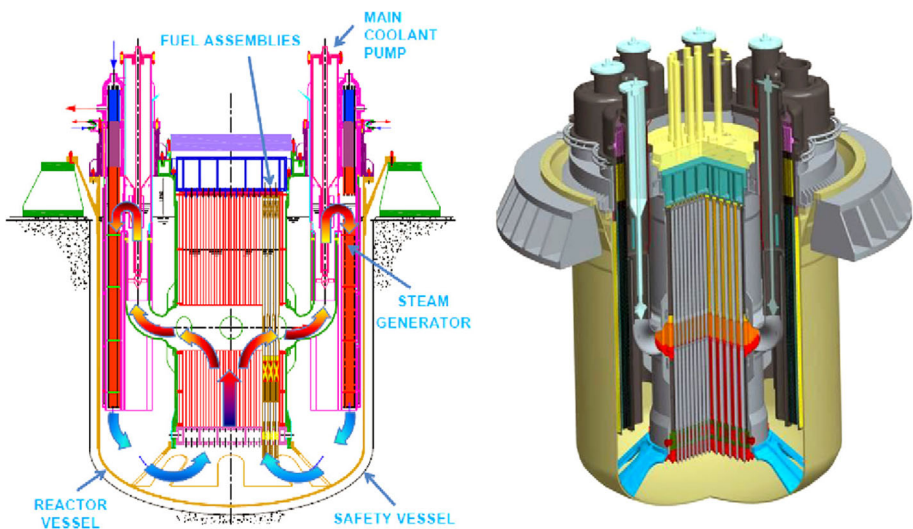
Fig. 1 ALFRED nuclear power plant layout

Fig. 2 ALFRED core configuration: 171 FAs (57 inner low enriched in orange, 114 outer high enriched in blue); 108 dummy assemblies in green; 12 outer CR; and four inner SR assemblies in red
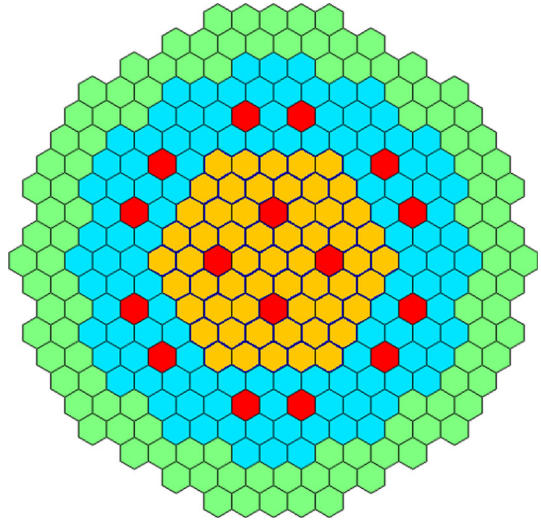
Table 1 ALFRED core main parameters

Thermal power	300 MW$_{th}$
Coolant mass flow rate	25,984 kg/s
Fuel type	MOX
Clad material	15–15 Ti
Max linear power	350 W/cm
Coolant inlet temperature	400 °C
Coolant outlet temperature	480 °C
Active height	60 cm
Active diameter	330 cm

cold pool into the core and is collected in a plenum (hot collector) to be delivered to SGs. After leaving the SGs, the coolant enters the cold pool through the cold leg and returns to the core.

The ALFRED core is composed by wrapped hexagonal fuel assemblies (FAs) with pins arranged on a triangular lattice (Fig. 2). The 171 FAs are organized into two radial zones with different enrichment (MOX enriched at 21.7 and 27.8% for the inner and outer zone, respectively), in order to radially flatten the thermal power. The surrounding two rows of dummy elements serve as reflector. Two different and independent control rods systems have been foreseen, namely control rods (CRs) and safety rods (SRs). Power regulation and reactivity swing compensation during the cycle are performed by the former, while the simultaneous use of both is foreseen for scram purposes, assuring the required reliability for a safe shutdown [4].

In Table 1, the major nominal parameters employed as input data to implement the core model are presented.

3 Multiphysics model

Neutronics and thermal-hydraulics interaction in the core needs the integration of stochastic calculations for neutron motion with computational fluid dynamics simulations. In the present study, neutronics is solved using Serpent, a continuous-energy Monte Carlo particle transport code [5], whereas thermal hydraulics is modeled with OpenFOAM, a C++ toolbox for the solution of continuum mechanics problems using finite volume method [6].

Serpent, given the temperatures of materials and the lead density, updates cross sections, solves the neutron transport in the system and returns the power distribution. In turn, Open-FOAM receives the power as input and updates material temperatures and the coolant density. The data exchange between the two codes is achieved by an iterative schemes, implemented in the same calculation environment [7]. Iteration scheme is described as follows:

– Initial spatially uniform temperature for every material and uniform lead density;
– Solve neutron transport with Serpent to compute power distribution;
– Run OpenFOAM with the current power to update temperatures and coolant densities;
– Iterate from the second step until convergence.

Simulations are set imposing the steady-state conditions of the reactor at the beginning of cycle (BOC). This implies mainly the use of atomic concentration of the fresh fuel and the position of control and safety assemblies in the BOC, which are partially inserted in the core. Remind that the withdrawn position of control rods is below the core.

3.1 Neutronics

The criticality calculation run in this work is based on the Serpent model developed at Politecnico di Milano by Stefano Lorenzi. Neutrons are transported throughout the whole reactor: The model includes the core active region, lower and upper plena and structural materials. A plot of the computational domain for the neutronic model is shown in Fig. 3.

Photon transport is not described in the present work. Furthermore, Serpent DBRC and $S(\alpha, \beta)$ scattering laws are not considered, since their utilization on fast systems can be neglected.

Material temperatures and coolant densities in the active region are updated according to the output files printed by the OpenFOAM simulation. As far as the evaluation of nuclide cross sections is concerned, instead of pre-calculating them beforehand for every temperature appearing in the system, cross sections are computed on the fly during the neutron transport by means of the TMS (target motion sampling) temperature treatment [8]. This method reduces significantly the memory consumption and the computational efforts in evaluating temperature dependencies of cross sections.

Specifically, the fuel is divided radially into three iso-volume zones, as shown in Fig. 4, to get a more accurate computation of the cross-sectional temperature dependencies. Moreover, the lead mass density variation is also taken into account.

The main outcome is the volumetric power distribution for each volume cell printed in files readable by OpenFOAM.

Furthermore, the Monte Carlo code is modified in order to print the absolute and the relative standard deviations of the volumetric powers.

The simulation parameters of the Serpent criticality calculations are reported in Table 2.

Neutron transport simulations are performed using JEFF-3.1.1 library for the cross sections of materials [9].
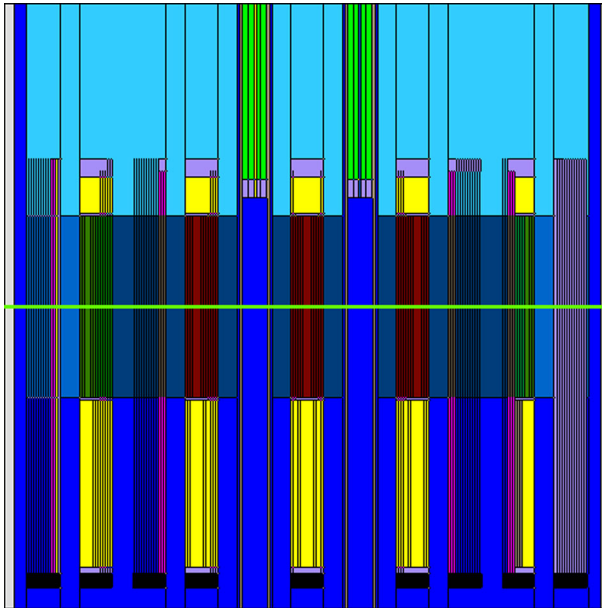
Fig. 3 Plot of computational domain section in the *x–z* plane for the neutronic modeling. Green line in the figure center visualizes the position of the *z* axis

Fig. 4 Section of the fuel pin: lead in blue, cladding in gray, gap in green, fuel (three zones) in red and internal void in yellow
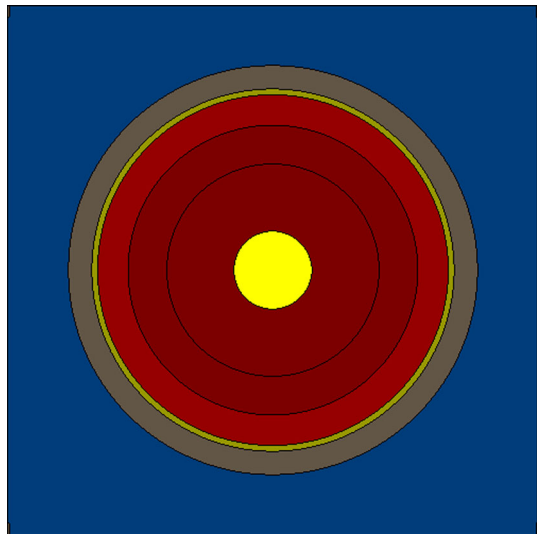
Table 2 Criticality calculation parameters

Neutron population	10, 000
Active cycles	5000
Inactive cycles	500

3.2 Thermal hydraulics

Although the neutron transport is described within the entire reactor, the thermal-hydraulics behavior of the coolant and other in-core material temperatures are computed solely within the active zone fuel assemblies (FAs).

The computational domain is based on a coarse mesh, whose structure reproduces the hexagonal lattice of the FAs. Each fuel assembly is split, in the cross section, into six equilateral triangles (Fig. 5a) and axially in 30 prisms (Fig. 5b). A convergence study of the mesh grid is performed varying the number of axial cells. The analysis of the convergence, along with the study of the most suitable numerical and discretization schemes, and the selection of appropriate iteration algorithms are important pieces on any CFD study. Nonetheless, the focus of the present work is on the coupling approach, rather than the numerical issues of single-physics modeling.

The whole computational domain is shown in Fig. 5c. It is remarked that assemblies containing control, safety and dummy rods are not part of the model domain for thermal-hydraulics calculations.

In order to compute lead temperatures in core active zone, pin bundles within each FA are treated as a porous medium and the steady-state energy equation is then solved. Neglecting the diffusion term, the energy equation implemented in the thermal-hydraulics code is the following

$$\rho c_p \bar{U}_{\text{Darcy}} \cdot \nabla T = P_{\text{vol}}, \tag{1}$$

where ρc_p is the volumetric heat capacity (J/m^{3}K) of lead and $\bar{U}_{\text{Darcy}}$ is the fluid flow Darcy velocity, computed as

$$\bar{U}_{\text{Darcy}} = \frac{\bar{U}}{\chi_{\text{lead}}}. \tag{2}$$

χ_{lead} represents the fraction of lead in a volume cell (which is approximately 56%) and $\bar{U}$ is the lead velocity in a certain FA. The term in the RHS of Eq. (1) is the volumetric power (W/m^3) distribution, which is given as output of the neutronics Monte Carlo runs.

Density change of lead due to both temperature and thermal expansion of cladding is also computed and passed to the neutronic code.

As far as boundary conditions are concerned, it is imposed an inlet temperature of lead equal to the nominal 673 K (400 °C). Regarding the velocity field of the coolant, a constant upstream velocity vectors are set in the volume cells, whose magnitudes ($\bar{U}$) are defined according to cooling group map depicted in Fig. 6.

Once the lead temperatures are computed, the pin material (cladding, gap, fuel and inner void) temperatures, averaged on volume cells, are reconstructed analytically.

Firstly, the outer cladding temperature is computed knowing the heat flux at the outer cladding surface (q_{co}) and assuming a lead-cladding heat transfer coefficient (HTC):

$$T_{\text{outerClad}} = T_{\text{lead}} + \frac{q_{co}}{\text{HTC}}. \tag{3}$$

The heat transfer coefficient is based on the Ushakov's correlation for the Nusselt number Nu for triangular rod bundles [10].

As far as the heat transfer in the cladding is concerned, the only relevant phenomenon is the radial conduction. Assuming constant conductivity, the inner cladding temperature can be found as
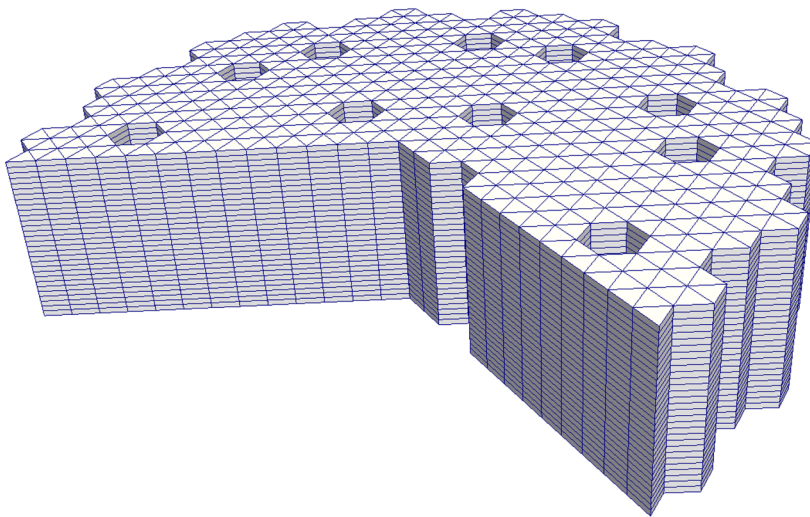
$$T_{\text{innerClad}} = T_{\text{outerClad}} + \frac{r_{co} \ln(r_{co}/r_{ci})}{\lambda_{\text{clad}}} q_{co}, \tag{4}$$
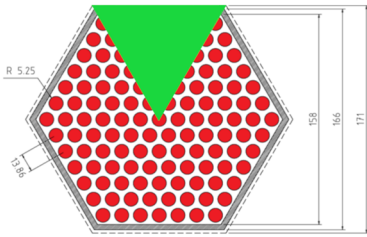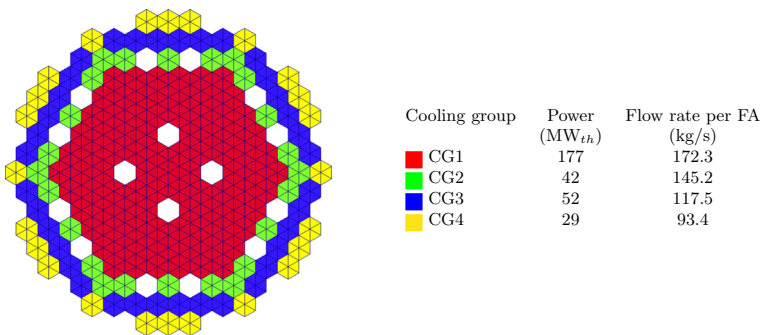
(a) Cross section subdivision of a FA.
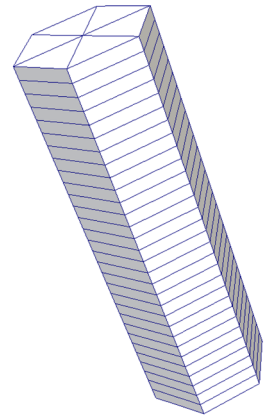
(b) Mesh of a single FA.

(c) Section of the entire computational domain.

Fig. 5 Computational domain for thermal-hydraulics simulations

Cooling group	Power (MW$_{th}$)	Flow rate per FA (kg/s)
CG1	177	172.3
CG2	42	145.2
CG3	52	117.5
CG4	29	93.4

Fig. 6 Cooling group map of ALFRED. On the right, the legend reports the mass flow rate of lead in each FA and the power produced per group

where r_{ci} is the inner cladding radius. The cladding temperature is computed as the mean value between the outer and the inner temperatures.

Concerning the gap, mean fuel performances at the BOL conditions are taken into account to model the heat transfer phenomena between fuel and cladding. (Gap thickness reduction due to fuel cracking is not modeled) [11]. Therefore, a constant conductance is assumed, as done for the cladding.

Regarding the fuel pellet, a temperature radial profile can be retrieved solving the radial heat conduction with a known volumetric power source and a constant thermal conductivity.

The fuel region is then divided into three iso-volume zones, as depicted in Fig. 4. From the radial profile, three fuel temperatures are picked corresponding to zones defined above. Concluding from the OpenFOAM simulations, temperatures of lead, cladding and fuel are obtained, which are average values over the computational cells.

4 Results

4.1 Convergence study

The change in the power generated in the central FA is controlled at the end of each Monte Carlo run in order to check the coupling convergence. After the second iteration, the relative change of power in the central FA is under 2 %. This is due to both the low value of the dominance ratio of ALFRED core and the role of lead as coolant, whose impact on neutron economy is considerably lower with respect to water-cooled reactors.

As far as the convergence of Monte Carlo simulations is concerned, a root mean square of standard deviation of volumetric powers is computed and plotted as function of the number of active cycles (Fig. 7). The standard deviation decreases as the inverse of the square of the active cycle number, which confirms the good convergence of the Serpent simulations.

4.2 Main results and plots

Lead temperature rises from the lower inlet surface, where it is imposed an inlet value of 673 K, to the upper outlet surface. The average outlet temperature is about 758 K that means an average temperature rise in the core of 85°.

Fig. 7 Convergence of Monte Carlo run: volumetric power standard deviation versus the number of active cycles. The inverse square root scaling is in red
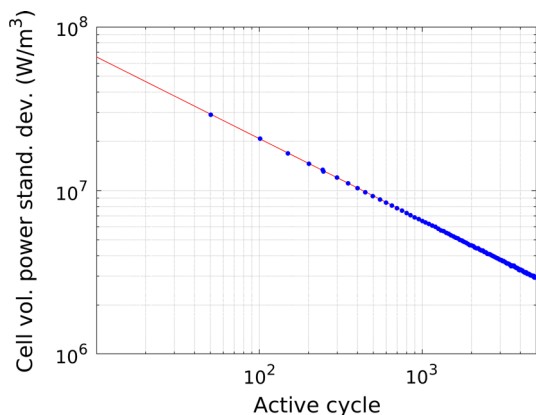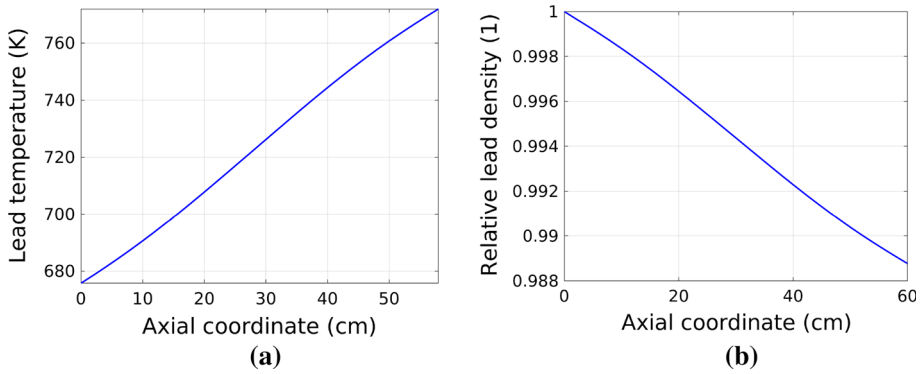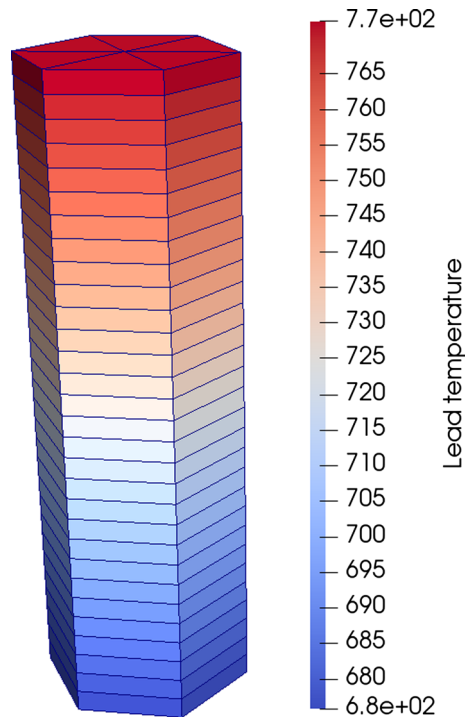
Fig. 8 Temperature (**a**) and relative mass density (**b**) axial profile of lead in the central FA

**Fig. 9** Lead temperature of the central FA (Kelvin)

The temperature axial profile in the central FA is depicted in Fig. 8a. In this plot, the temperature value for a certain height is computed as the mean value of the six cell values in the xy plane (Fig. 9). On the contrary, the relative density decreases of about 1%, as depicted in Fig. 8b.

Once the lead temperatures for every volume cells are known, pin material temperatures are reconstructed analytically as explained above. By referring again to the central FA, Fig. 10a shows the axial profiles of lead, outer cladding and pellet temperatures. In particular, the chromatic sequence of reds, from the lightest to the darkest, corresponds to the outer pellet, the three iso-volume zones and the inner pellet temperatures, respectively.
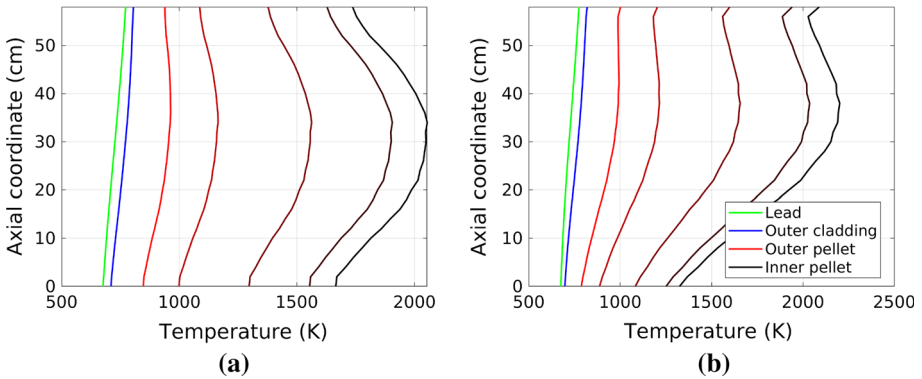
Fig. 10 Axial profile of, from the left, respectively, lead, outer cladding, outer pellet, three fuel zones and inner pellet temperatures of the central FA (**a**) and of the FA with maximum linear power (**b**)
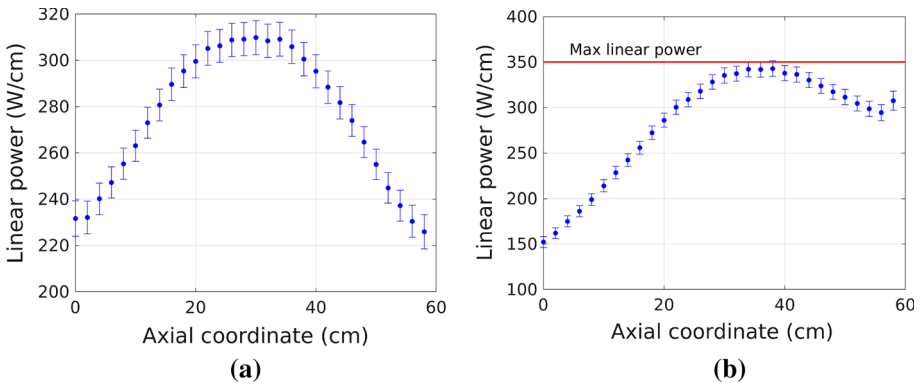
Fig. 11 Pin average linear power of central FA (**a**) and FA with maximum value of linear power (**b**). Error bars refer to 1-sigma uncertainty

Figure 10b refers instead to the FA with maximum fuel linear power, which is located in the innermost round of the higher enriched zone, next to a control assembly. The axial profile is shifted upward, since the control assembly is partially inserted in BOL conditions, from below.

As far as the power generation is concerned, the linear power, averaged over all pins in the FA, is computed and plotted in Fig. 11. The profile shows consistent values if compared to results available in the literature [12]: Peak value in the central FA is around 320 W/cm. Furthermore, the maximum value of linear power over the whole reactor does not overcome 350 W/cm, which is the threshold prescribed by design [3].

Inner pellet temperatures reflect the trend of the linear power, as it can be observed by comparing Figs. 11a, b with 10a, b, respectively.

Figure 12 reports a section of the computational domain where the lead temperature and inner pellet (which coincides with the maximum fuel temperature within a cell) are depicted . The maximum fuel temperature over the whole domain is about 2200 K, in agreement with the main technological constraint for the ALFRED core design [13].

The last pictures regard the volumetric power distribution within the core. Figure 13a shows the main outcome of the Monte Carlo transport calculation, which is the volumetric power
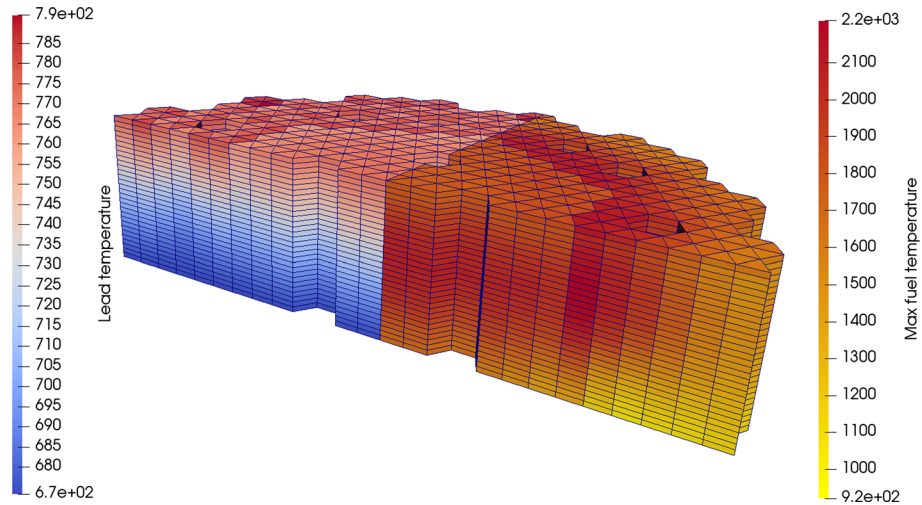
Fig. 12 Lead and maximum fuel temperature distributions (Kelvin)

cell by cell. The two different enriched zones can be individuated, and moreover, the reader can easily visualize the fuel assembly with maximum linear power discussed above.

Furthermore, the Serpent code is modified to print the statistical errors on the volumetric power in order to be depicted graphically. On the right half of the domain in Fig. 13b, the relative standard deviation is shown. It acquires the lowest values in the core center, while highest ones in the core borders, where the fewest number of scores is collected. Nevertheless, the absolute error remains small everywhere with respect to the corresponding expected value, as it is shown in Fig. 13b.

5 Scalability analysis

The last part of the paper is dedicated to investigate how the Serpent–OpenFOAM coupled application for ALFRED core scales with increasing workload. Measuring the scalability of a certain application indicates how efficient is the latter one in using increasing number of parallel cores [14].

There are basically two ways to measure this property. In the hard scalability, the problem size is fixed, while the number of processors increases. Hard scalability is used when applications are CPU-bounded. However, in the soft scaling approach, the computational load assigned to each CPU is kept constant. Therefore, computationally larger problems are solved with additional processors. Soft scaling is used for memory-bounded applications.

To test the performance of the Serpent–OpenFOAM coupling for ALFRED, soft scalability approach is adopted. Simulations are performed using Intel(R) Xeon Phi(TM) CPU 7210 @ 1.30GHz, provided by the computational machine platform in the frame of OCAPIE (Ottimizzazione di CAlcolo Parallelo Intensivo Applicate a problematiche in ambito Energetico) project. Computational scalability is tested by monitoring the time needed to complete one coupled iteration, varying the threads and keeping constant the number of inactive and active cycles.

(a)

(b)
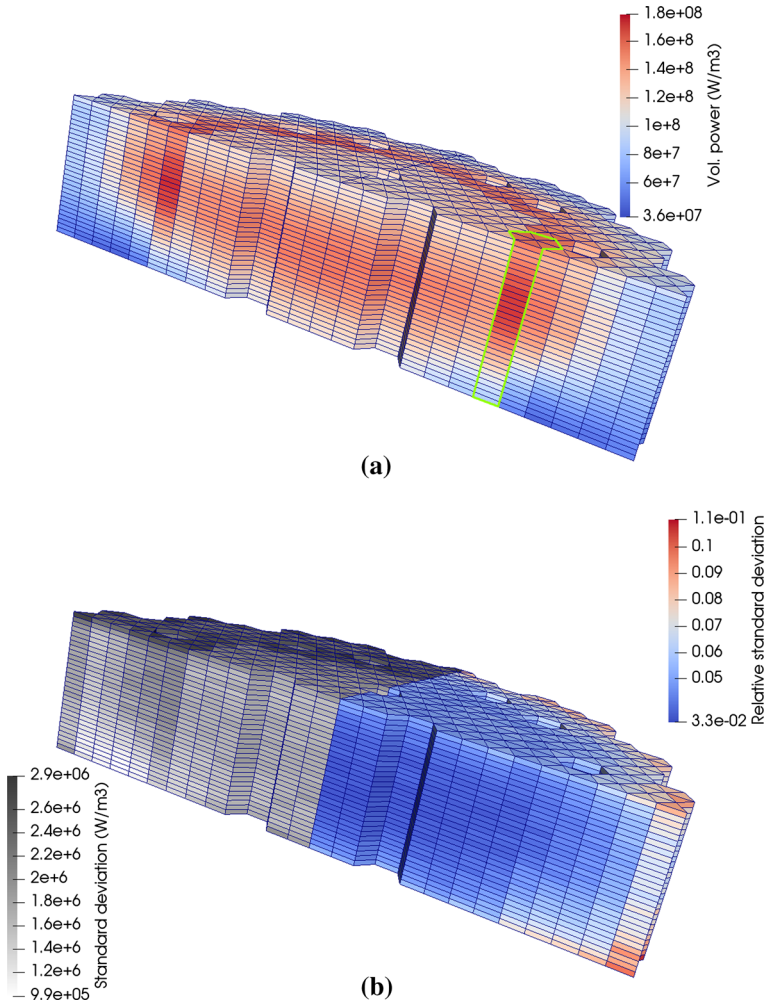
Fig. 13 Distribution of volumetric power (**a**) and associated relative and absolute errors (**b**). It is highlighted the FA with maximum power generation in green

Simulations with 1, 8, 16, 24, 32, 40, 48, 56 and 64 threads on a single HPC cluster are launched, increasing the neutron population per cycle, respectively. Moreover, parallel runs with the HPC cluster are computed by passing the job schedulers, in order to better handle the allocated computational resources for the purpose of the scalability test.

Results of the scalability tests are reported in Table 3 and depicted in Fig. 14. The figure above shows that the expected linear scaling is achieved, since the run time stays constant, while the computational size of the problem increases linearly with respect to the number of threads. Finally, a soft scalability efficiency can be defined as the ratio between the running time with one single unit and the time to perform the simulation with more than one units. It is approximately 90 %.

Finally, this result confirms the excellent scalability performance of Monte Carlo simulations and its application to neutron transport calculations.

Table 3 Soft scalability analysis for the Serpent–OpenFOAM coupling study of ALFRED

Number of threads	1	8	16	24	32	40	48	56	64
Neutron pop. per cycle	417	3333	6667	10,000	13,333	16,667	20,000	23,333	26,667
Running time (min)	787.5	855.6	840.7	860.2	865.5	874.2	867.5	865.3	872.6

Fig. 14 Soft scalability results: CPU running time versus the number of threads used
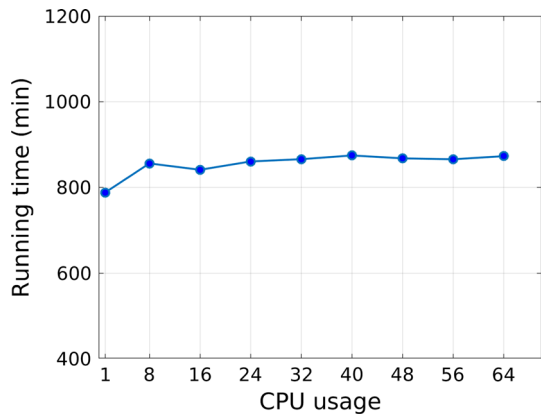
6 Conclusions

In this paper, a multiphysics model is proposed for the analysis of the ALFRED core, the LFR technology demonstrator in the frame of LEADER project. Neutronics is modeled with a stochastic description of the neutron transport within the whole core, while thermal hydraulics is solved with a coarse-mesh approach to compute average temperature distributions of lead, cladding and fuel within fuel assemblies. Cross sections of nuclides are evaluated on the fly, during the Monte Carlo runs, taking into account the real temperatures of materials, which are substantially not uniform throughout the core.

Results are in agreement with the design parameters and other related calculations reported in the literature. Moreover, the model adopts the TMS temperature treatment for evaluating cross-sectional on the fly on non-uniform material temperature distributions to drastically reduce the computational effort and memory requirement.

Future activities will be devoted to the perturbation analysis of nuclear data. Perturbation theory can be implemented in conjunction with the on-the-fly temperature treatment of cross sections, in order to get sensitivity coefficients taking into account temperature non-uniformity with relatively low computational cost. One of this application will be to investigate the spatial variation of the effective multiplication factor lead density sensitivity coefficient, which changes sign in the ALFRED core. (It is positive in the inner region, while it is negative in the outer one.) [15]

Other future developments will regard the extension of the present model to describe transients. Monte Carlo time-dependent solution, performed with Serpent, can be addressed with the dynamic simulation mode, which keeps the simulated population size within reasonable limits and corrects the neutron statistical weights at the end of each time interval.

References

1. A Technology Roadmap for Generation IV Nuclear Energy Systems (GIF, 2002) Technical Report GIF-002-00
2. LEADER project. www.leader-FP7.eu
3. M. Frogheri, A. Alemberti, L. Mansani, The Lead Fast, Reactor: Demonstrator (ALFRED) and ELFR Design, International Conference on Fast Reactors and Related Fuel Cycles: Safe Technologies and Sustainable Scenarios (FR13), Paris, France, (2013)
4. G. Grasso, C. Petrovich, D. Mattioli, C. Artioli, P. Sciora, D. Gugiu, G. Bandini, E. Bubelis, K. Mikityuk, The core design of ALFRED, a demonstrator for the European lead-cooled reactors. Nucl. Eng. Des. **278**, 287–301 (2014)
5. J. Leppänen, The Serpent Monte Carlo code: status, development and applications in 2013. Ann. Nucl. Energy **82**(2015), 142–150 (2013)
6. OpenFOAM. www.openfoam.org
7. J. Leppänen, T. Viitanen, V. Valtavirta, Multi-physics coupling scheme in the Serpent 2 Monte Carlo code. Trans. Am. Nucle. Soc. **1074**, 1165–1168 (2012)
8. T. Viitanen, J. Leppänen, Target motion sampling temperature treatment technique with elevated basis cross section temperatures. Nucl. Sci. Eng. **177**, 77–89 (2014)
9. The JEFF-3.1.1 Nuclear Data Library, 2009. Technical Report JEFF report 22, OECD/NEA Data Bank
10. P.A. Ushakov, A.V. Zhukov, N.M. Matyukhin, Heat transfer to liquid metals in regular arrays of fuel elements. Teplofiz. Vysok. Temp. **15**(5), 1027 (1977)
11. L. Luzzi, A. Cammi, V. Di Marcello, S. Lorenzi, D. Pizzocri, P. Van Uffelen, Application of the TRANSURANUS code for the fuel pin design process of the ALFRED reactor. Nucl. Eng. Des. **277**, 173–187 (2014). https://doi.org/10.1016/j.nucengdes.2014.06.032
12. E. Bubelis, K. Mikityuk, Plant data for the safety analysis of the ETDR (ALFRED), PSI/KIT (including contributions from ANSALDO, ENEA, EA, CEA, SRS) Technical Report TEC058-2012 (2012)
13. C. Petrovich, K. Mikityuk, F. Manni, D. Gugiu, G. Grasso, ALFRED core. Summary, synoptic tables, conclusions and recommendations, ENEA, UTFISSM-P9SZ-006 (2013)
14. The Weak Scaling of DL_POLY 3. STFC Computational Science and Engineering Department. Archived from the original on March 7, 2014. Retrieved March 8 (2014)
15. M. Aufiero, M. Martin, M. Fratoni, E. Fridman, S. Lorenzi, Analysis of the coolant density reactivity coefficient in LFRs and SFRs via Monte Carlo perturbation/sensitivity, Conference: PHYSOR 2016 At Sun Valley, ID, USA (2016)